FRONTIERS OF PHYSICS

RESEARCH ARTICLE
Volume 19 / Issue 3 / 32206 / 2024

Unidirectional propagation of water waves near ancient Luoyang Bridge

Linkang Han[1,2], Qilin Duan[2], Junliang Duan[2], Shan Zhu[2], Shiming Chen[2], Yuhang Yin[2], Huanyang Chen[1,2,3,†]

1 Shenzhen Research Institute of Xiamen University, Shenzhen 518000, China
2 Department of Physics, Xiamen University, Xiamen 361005, China
3 Key Laboratory of Underwater Acoustic Communication and Marine Information Technology of the Ministry of Education, Xiamen University, Xiamen 361005, China
Corresponding author. E-mail: †kenyon@xmu.edu.cn
Received November 28, 2023; accepted April 12, 2024

ABSTRACT

Metasurfaces and metagratings offer new platforms for electromagnetic wave control with significant responses. However, metasurfaces based on abrupt phase change and resonant structures suffer from the drawback of high loss and face challenges when applied in water waves. Therefore, the application of metasurfaces in water wave control is not ideal due to the limitations associated with high loss and other challenges. We have discovered that non-resonant metagratings exhibit promising effects in water wave control. Leveraging the similarity between bridges and metagratings, we have successfully developed a water wave metagrating model inspired by the ancient Luoyang Bridge in China. We conduct theoretical calculations and simulations on the metagrating and derive the equivalent anisotropic model of the metagrating. This model provides evidence that the metagrating has the capability to control water waves and achieve unidirectional surface water wave. The accuracy of our theory is strongly supported by the clear observation of the unidirectional propagation phenomenon during simulation and experiments conducted using a reduced version of the metagrating. It is the first time that the unidirectional propagation of water waves has been seen in water wave metagrating experiment. Above all, we realize the water wave metagrating experiment for the first time. By combining complex gratings with real bridges, we explore the physics embedded in the ancient building — Luoyang Bridge, which are of great significance for the water wave metagrating design and provide a new method for analyzing the effects of water waves on bridges. At the same time, this discovery also provides a new idea for ocean cargo transportation, ocean garbage cleaning, and the development and protection of ancient bridges.

Keywords Luoyang Bridge, unidirectional propagation, water wave metagratings, equivalent anisotropic model

Higher Education Press

https://doi.org/10.1007/s11467-024-1411-x

1 Introduction

Water waves are ubiquitous in our daily lives, representing one of the most common forms of waves. They are mechanical waves that widely exist on the surface of various waters, and the restoring force is provided by gravity [1, 2]. The investigation of water wave scattering, diffraction, and decay as well as the development of novel techniques for water wave control are hot topics in the field of water wave mechanics for a long time [2, 3]. In the past ten years, photonic crystals [4–7], metamaterials [8–11] and metasurfaces/metagratings [12–16] have demonstrated significant success in the control of electromagnetic waves. Consequently, researchers have extended these structures and methods into water wave systems (new corresponding relationship can be seen in Section 1 of the Electronic Supplementary Materials (ESM) [17]), such as employing photonic crystals to achieve negative refraction [18] and self-collimation [19] of water waves. Additionally, the utilization of metamaterials has enabled advancements in water wave control, including cloaking [20, 21], rotation of water waves [22], focusing [23, 24] and concentration [25]. Furthermore, periodic metamaterials have shown promise in achieving extraordinary effects in water wave systems, which can be applied to achieve negative gravity [44], surpass the upper limit of water wave velocity [26], etc. However, the application of metasurfaces and metagratings in water waves control, especially in experiments, is still limited and infrequent. In our previous work, we have theoretically proved that the metagratings can effectively isolate water waves and provide protective measures for buildings [27], while no experiments have been conducted so far. Therefore, conducting experiments on water wave metagratings is a highly worthwhile and timely compelling topic for exploration.

Metasurfaces and metagratings are a new type of artificial subwavelength materials that have been very popular in recent years, which provide a new method for wave field control and enabling the implementation of interesting functions [12–16]. Some notable functions include extraordinary optical diffraction [28], asymmetric Perfect Diffraction [29], negative diffraction [30], large numerical aperture focusing [31], broadband holographic display [32], holographic photoelectric detection [33], angular asymmetric absorption [34], non-scattering manipulation of abnormal reflection and refraction [35–37], reversal of transmission and reflection [38], and extension of the incident angle to several discrete angles [39]. Most metasurfaces are typically designed based on abrupt phase change and resonance, however, the propagation of water waves is often associated with substantial loss. Thus, the utilization of abrupt phase changes and resonant structures in metasurfaces will further deepen the loss of the water wave, resulting in poor water wave control effect. This may be a crucial reason why metasurfaces have not been extensively employed for water wave control. However, through our research, we have discovered that certain non-resonant metagratings exhibit minimal loss for water waves while demonstrating good control capabilities. In this article, building upon the previous theoretical work, specifically the utilization of the Luoyang Bridge metagrating model for water wave control [27], we proceed to design a novel non-resonant metagrating model to investigate and comprehend the underlying mechanism of controlling water waves through metagratings.

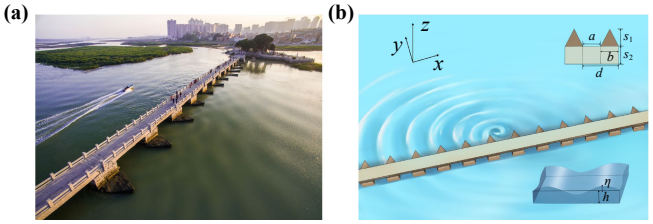

Fig. 1 Luoyang Bridge and its metagrating model. **(a)** Realistic terrain scene of Luoyang Bridge [40]. **(b)** The vortex water source excites a unidirectional surface water wave near the metagrating (the detailed structure diagram of the metagrating is shown at the upper right corner of the picture and the enlarged view of the vertical displacement of water surface η and the static water depth h (or average water depth) is shown at the lower right corner).

Luoyang Bridge is an ancient bridge located in Quanzhou, China (see Fig. 1(a) [40]), which has a history of more than 1000 years, stretching over 1000 meters and featuring an array of 46 pillars [41]. Remarkably, the unique ship-like pillar structures give Luoyang Bridge some unique physical characteristics, such as eliminating water waves [27, 42]. Through the research of the metagrating model of Luoyang Bridge, we find another intriguing phenomenon: vortex water waves can excite unidirectional surface water wave near the metagrating, as shown in Fig. 1(b).

We can see that the vertical displacement of the vortex water wave (excited by the rotating propeller) at the right side of the source is greatly weakened, while at the left side of the source is enhanced, forming a unidirectional surface water wave. To comprehend the origins of this phenomenon, we conduct rigorous theoretical calculations and numerical simulations. Furthermore, we validate this phenomenon in experiments.

2 Theoretical analysis and numerical simulation

If we consider linear, inviscid, and irrotational water waves in an infinite extent of water of constant depth h, its governing equation is [2, 43]

$$\nabla \cdot (u \cdot \nabla p) + \frac{\omega^2}{g} p = 0, \tag{1}$$

where u is the reduced water depth, $u = \tanh(kh)/k$ [44], p is the hydrostatic pressure of water surface ($p = \rho g \eta$), ρ is the fluid density, g is the gravitational acceleration, η is the vertical displacement of the water wave, and the nonlinear dispersion of water waves is [45, 46]

$$\omega = \sqrt{gu}k, \tag{2}$$

where ω is the angular frequency and k is the propagation wave number of water wave.

Then we first write the vertical displacement expression of the vortex water wave in the x–y plane as $\eta(x, y) = H_1(k_0 r)\, \mathrm{e}^{\mathrm{i}\theta} = \int \tilde{\eta}(k_x, y) \mathrm{e}^{\mathrm{i}k_x x} \mathrm{d}k_x$, where

$$\tilde{\eta}(k_x, y) = \frac{1}{\pi k_0} \left(\mathrm{i} \frac{k_x}{k_y} \mp 1 \right) \mathrm{e}^{\mathrm{i}k_y |y - y_{\text{source}}|}. \tag{3}$$

$\tilde{\eta}(k_x, y)$ is spatial Fourier transform of $\eta(x, y)$, H_1 is the Hankel function of the first kind, k_x and k_y are the wave number in the x and y direction, $k_y = (k_0^2 - k_x^2)^{1/2}$ and $k_0 = 2\pi/\lambda$. Here λ is the wavelength, r and θ are cylindrical coordinate systems, and $r\cos\theta = x$, $r\sin\theta = y$. The minus and plus signs in Eq. (3) respectively correspond to $y > y_{\text{source}}$ and $y < y_{\text{source}}$, where y_{source} is the location of the source (e.g., a vortex water wave).

We assume that the wave number of the water wave propagating along the positive direction and negative direction of x-axis are $k_x > 0$ and $k_x < 0$ respectively. Because the wave source is located at $(0, y_{\text{source}})$ in Fig. 1(b), we can use the left part and right part of the wave source to represent $k_x < 0$ and $k_x > 0$ respectively. When $|k_x| > k_0$, $k_y = \mathrm{i}\sqrt{k_x^2 - k_0^2}$, then we bring it into Eq. (3) to get

$$\tilde{\eta}(k_x, y) = \frac{1}{\pi k_0} \left(\frac{k_x}{\sqrt{k_x^2 - k_0^2}} \mp 1 \right) \mathrm{e}^{-\sqrt{k_x^2 - k_0^2}|y - y_{\text{source}}|}. \tag{4}$$

It can be seen from Eq. (4) that η is an evanescent wave in the y direction, and in the region of $y < y_{\text{source}}$ [corresponding to plus signs in Eq. (4)], the vertical displacement of the evanescent wave components are enhanced in the part of $k_x > 0$ (on the right part of wave source), while for the part of $k_x < 0$ (on the left part of wave source), the evanescent wave components are mutually eliminated. Therefore, by making the propagation wave number of the evanescent wave in the x direction meeting $|k_x| > k_0$, it is possible to excite the unidirectional surface water waves [47]. Can the metagrating excite surface wave with $|k_x| > k_0$? Let us analyze and calculate it below.

Due to the complex structure of metagrating shown in Fig. 1(b), it is difficult to carry out accurate analytical calculation at present. We first simplify it into a structure of periodic rectangular grating (which is directly called SPRG later) as shown in Fig. 2(a), and the top view of the specific dimensions of the two adjacent rectangles is shown in the upper right corner of Fig. 2(a), the length of each rectangle is $s_1 + s_2 = 11$ m, the width is $b = 5$ m, and the distance between two rectangles is $a = 6$ m, that is, the length of a unit cell is $d = a + b = 11$ m. We first solve the dispersion relation of the excited surface mode of SPRG as [48] (the derivation is in Section 1 of the ESM)

$$k_x = \frac{\sqrt{d^2 \left[\mathrm{e}^{\mathrm{i}k_0(s_1+s_2)} + 1\right]^2 - a^2 \left[\mathrm{e}^{\mathrm{i}k_0(s_1+s_2)} - 1\right]^2}}{d\left[1 + \mathrm{e}^{\mathrm{i}k_0(s_1+s_2)}\right]} k_0. \tag{5}$$

Through calculations, we find that SPRG can excite the surface mode of water waves, localize the water waves on its surface, form surface water waves, so the x-direction propagation wave number $|k_x|$ will become large, exceeding k_0, thereby unidirectional propagation of water waves can be realized. Analytical calculation and numerical simulation verification are carried out below.

We cannot simulate the infinitely long SPRG in a limited space, so we can make the SPRG be equivalent to an anisotropic water layer, if the reduced water depth in the area of $y > -6$ m and $y < -17$ m in Fig. 2(b) is set as u_0, then the equivalent parameters of the anisotropic water layer is $u_x = 0, u_y = a/d * u_0, g = d/a * g_0$ (the derivation is in Section 1 of the ESM). Then, the dispersion relation of the excited surface mode of the anisotropic water layer can be solved as follow (the derivation is in Section 1 of the ESM):

$$k_x = \frac{\sqrt{d^2 \left(\mathrm{e}^{\mathrm{i}k_0(s_1+s_2)} + 1\right)^2 - a^2 \left(\mathrm{e}^{\mathrm{i}k_0(s_1+s_2)} - 1\right)^2}}{d\left(1 + \mathrm{e}^{\mathrm{i}k_0(s_1+s_2)}\right)} k_0. \tag{6}$$

By comparing Eqs. (5) and (6), we can find that the dispersion relation expressions of the surface modes excited by the equivalent anisotropic water layer and the SPRG are exactly the same, which analytically proves that this equivalence is feasible. Then we bring the equivalent anisotropic water layer into the commercial software COMSOL Multiphysics for verification.

The simulation results are shown in Fig. 2(b). The area of the equivalent anisotropic water layer in Fig. 2(b) is within -17 m $< y < -6$ m, the wave source is at (0, 0), in order to satisfy the condition that surface waves appear on the metagrating: the wavelength is 4 times greater than that of the groove depth of the metagrating [$\lambda > 4(s_1+s_2)$], we set the wavelength around 46.4 m. This belongs to the case where the equivalent anisotropic water layer is located in the region of $y < y_{\text{source}}$. Eq. (4) should take the plus sign. From the field patterns in Fig. 2(b), it can be seen that in the equivalent

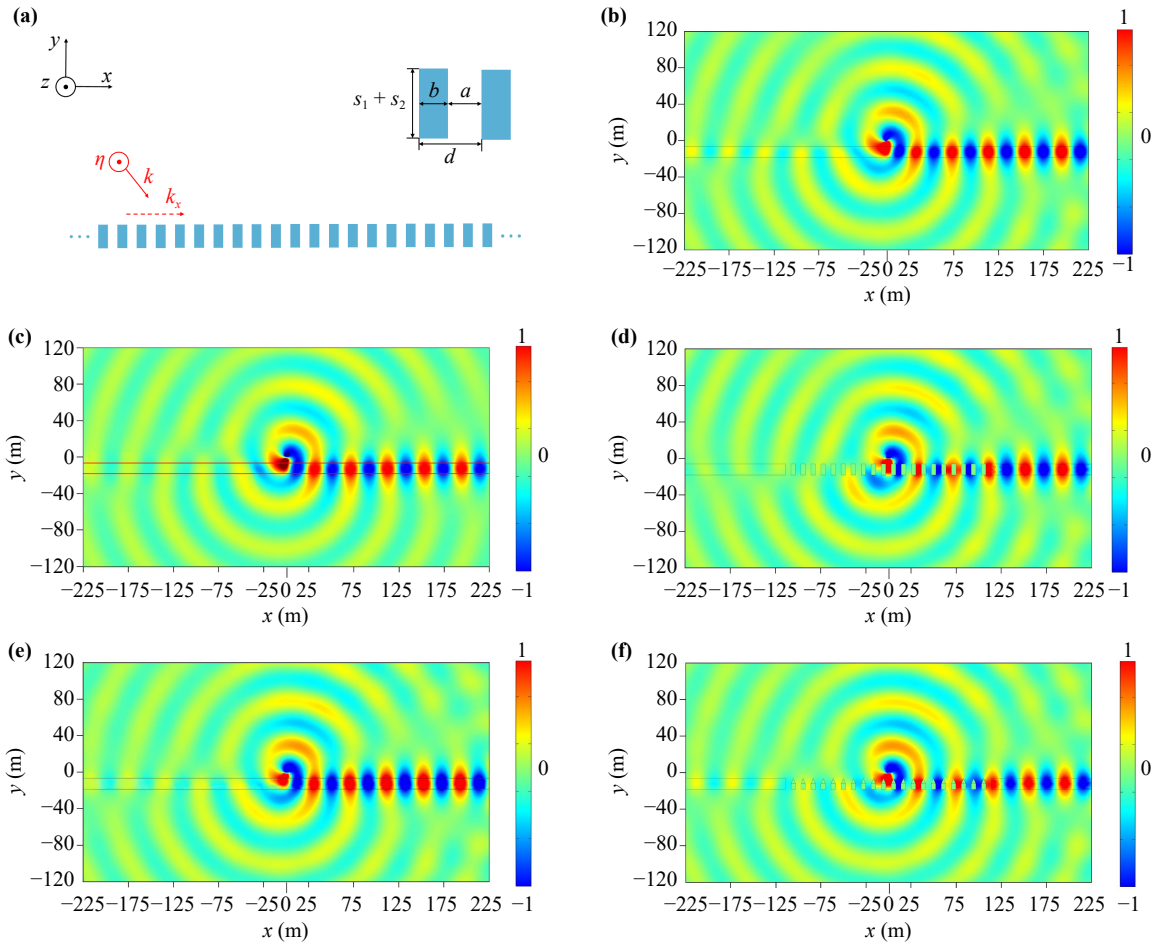

Fig. 2 Water wave field patterns of four equivalent models of Luoyang Bridge. **(a)** Schematic diagram of SPRG. The simulation **(b)** and the analytical solution **(c)** of field pattern of water wave excited by the equivalent anisotropic water layer of the SPRG. **(d)** The simulated field pattern of water wave excited by the spliced model of the SPRG. The simulated field pattern of water wave excited by the equivalent anisotropic gradient water layer **(e)** and the spliced model **(f)** of Luoyang Bridge.

anisotropic water layer, the vertical displacement of water wave in the left part ($k_x < 0$) is weakened, while in the right part ($k_x > 0$) is enhanced, forming a unidirectional surface water wave propagating to the right, which is in good agreement with the theory. Then we expand the vortex water wave in Fig. 2(b) by plane waves, solve the expression of water wave in each region analytically, and plot the field pattern of water wave corresponding to Fig. 2(b), as shown in Fig. 2(c) (the derivation is in Section 1 of the ESM). In order to distinguish from Fig. 2(b), the anisotropic water layer in Fig. 2(c) is marked with a solid red line. By comparing Figs. 2(b) and (c), we can find that the field patterns in Fig. 2(b) and Fig. 2(c) are almost identical, which also proves that our numerical simulation and analytical calculation are in good agreement with each other. With this equivalent anisotropic water layer, we can simulate an infinitely long SPRG. We can use the method of splicing the equivalent anisotropic water layer and the perfectly matched layer (PML) to the two sides of the SPRG to extend it infinitely (which is directly called splicing model later), and then the numerical simulation of the SPRG can be carried out accurately. The simulation results are shown in Fig. 2(d), where the area of the spliced model of the SPRG is $-17\,\mathrm{m} < y < -6\,\mathrm{m}$, the wave source is located at (0, 0), and the wavelength is 46.4 m. The simulation results show that Fig. 2(c) and Fig. 2(d) are highly similar. The wave source excites the surface water wave propagating to the right in the SPRG, and then enters the equivalent water layer and continues to propagate to PML. The vertical displacement of the water wave in the right part is enhanced, while in the left part is greatly weakened, thereby forming a unidirectional surface water wave, which proves that the SPRG can indeed excite a unidirectional surface water wave. In order to make our equivalent model closer to the real Luoyang Bridge, we introduce the anisotropic gradient water layer into the equivalent model. Then we

can write down a possible equivalent parameter of the equivalent gradient anisotropic water layer of the whole Luoyang Bridge by the layered method as follows (the derivation is in Section 1 of the ESM):

$$\overleftrightarrow{u}, g = \begin{cases} u_x = 0, u_y = \dfrac{(d + y + s_1 + 1)}{d} * u_0, g = \dfrac{d}{(d + y + s_1 + 1)} * g_0 & (-11\ \text{m} < y < -6\ \text{m}) \\ u_x = 0, u_y = \dfrac{a}{d} * u_0, g = \dfrac{d}{a} * g_0 & (-17\ \text{m} < y < -11\ \text{m}) \end{cases}, \tag{7}$$

where $u_0 = \tanh(k_0 h_0)/k_0$, $k_0 = 2\pi/\lambda$, the background water depth of real Luoyang Bridge is $h_0 = 3$ m, and the wavelength $\lambda = 46.4$ m.

The simulation result of equivalent anisotropic gradient water layer is shown in Fig. 2(e), in which the area of $-17\ \text{m} < y < -6$ m is the equivalent anisotropic gradient water layer, and the wave source is located at (0, 0) with wavelength $\lambda = 46.4$ m, which belongs to the case where the equivalent gradient water layer is located in the region of $y < y_{\text{source}}$. From the field pattern in Fig. 2(e), it can be seen that the vertical displacement of water wave in the left part ($k_x < 0$) in the equivalent gradient water layer is weakened, while in the right part ($k_x > 0$) is enhanced to form a unidirectional surface water wave propagating to the right. We extend the metagrating of Luoyang Bridge infinitely by the splicing method. Then we simulate and verify the splicing model, and the simulation result is shown in Fig. 2(f). The area of $-17\ \text{m} < y < -6$ m in Fig. 2(f) is the equivalent gradient water layer and the splicing model of metagrating, where the wave source is located at (0, 0), and the wavelength is still $\lambda = 46.4$ m. From the simulation results, it can be seen that Fig. 2(e) and Fig. 2(f) are highly similar, also forming a unidirectional propagation surface water wave, which proves that the metagrating can indeed excite a unidirectional propagation surface wave for water waves.

3 Experimental verifications

We then do some experiments to qualitatively observe the unidirectional propagation water wave excited near the metagrating. We print out a reduced metagrating with a 3D printer [reduced by 100 times compared to Fig. 1(b)], its structure diagram is shown in Supplementary Fig. S6(c) and its material is PLA plastic, and its structural dimensions are $a = 0.6$ cm, $b = 0.5$ cm, $d = 1.1$ cm, $s_1 = 0.5$ cm, and $s_2 = 0.6$ cm. The water depth in the experiment is 8 mm. The equipment used in the experiment is shown in Supplementary Figs. S6(a, b). A miniature propeller is used to excite the vortex water wave, we set its frequency f to 5.1 Hz, according to the dispersion relation of water waves Eq. (2), we can find that the corresponding wavelength λ is 4.64 cm, the impermeable rigid body is a reduced metagrating (in cyan), and the black sponges on the left and right sides are used to eliminate the reflection of water waves at outer boundaries (detailed structure could be seen in Section 2 of the ESM).

The experimental results are shown in Fig. 3. Figure 3(a) is a schematic diagram of the observation of experimental results. The light shines from above and projects the trajectory of the water waves onto the bottom screen to facilitate our observation. Therefore, the experimental results below are all projections of water waves. In order to highlight the role of metagratings, we design a set of control experiments as shown in Fig. 3(b). The sample of the control group is in the upper part, which is a flat plate without any structure. The sample of the experimental group is in the lower part, which is a reduced metagrating.

Due to the capillary effect of water, the projected area of the metagrating is larger than itself, making it difficult to observe the near-field surface water waves formed by vortex waves near the metagrating. However, when we carefully observe the simulation results in Fig. 2, we will find that obvious unidirectional phenomena can also be seen in the far field of 1 to 2 wavelengths near the wave source. This is because the field near the wave source is strong. Although the unidirectional surface water wave is evanescent wave, it can still propagate a certain distance. Therefore, we verify our conclusion by observing the unidirectional phenomenon in the far field near the wave source in the experiment.

Figure 3(c) shows the experimental results without metagrating. It can be seen that a complete vortex water wave (a counterclockwise rotating propeller) has the same vertical displacement on both sides of the water wave with a wavelength of 4.64 cm (with frequency 5.1 Hz).

Figure 3(d) shows the experimental results of the control group. The wavelength is still 4.64 cm, and the wave source (a counterclockwise rotating propeller) is put 0.6 cm away from the flat plate. It can be seen that the water wave on the left side of the wave source is strongly reflected after encountering the flat plate, and the vertical displacement of the water wave does not weaken at all.

Then we replace the flat plate with reduced metagrating, the experimental results are shown in Figs. 3(e) and (f). When the propeller rotates clockwise (counterclockwise), the vertical displacement of the water wave on the right (left) side of the wave source is weakened, forming a unidirectional surface water wave propagates to the left (right). At the same time, by comparing Figs. 3(d) and (f), we can see that compared with the

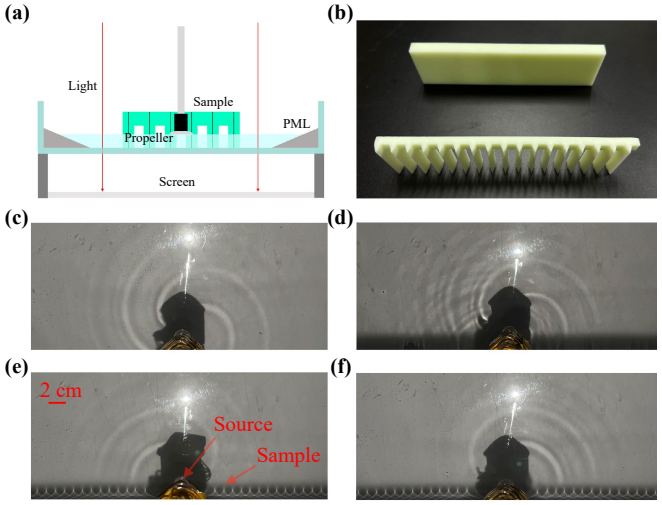

Fig. 3 Experimental results. **(a)** Side view of the experimental equipment. **(b)** The Sample of control (up) and experimental (down) group. **(c)** Vortex water wave excited by a rotating miniature propeller, the propeller is counterclockwise rotating. **(d)** Field pattern for the case when the rotating propeller is close (0.6 cm) to the flat plate. The propeller is counterclockwise rotating. **(e, f)** Field pattern for the case when the rotating propeller is close (0.6 cm) to the reduced metagrating. The propeller is (clockwise) counterclockwise rotating.

flat plate, the metagrating can significantly weaken the vertical displacement of the water wave on the left side of the wave source, proving that the metagrating can indeed excite unidirectional propagating surface water waves, which is in good agreement with our theory. [Figures 3(e) and (f) have corresponding videos in Section 2 of the ESM.]

We also conduct experiments near the real Luoyang Bridge. However, Luoyang Bridge is a protected area, we cannot conduct more systematic experiments, but some unidirectional effects can also be seen. The water depth near Luoyang Bridge is about 3 m, we use a ship to rotate in situ to excite a vortex water wave near Luoyang Bridge. Due to the complex water conditions near Luoyang Bridge, we slow down the frequency of the ship's rotation to 0.09 Hz (if the ship continues to slow down, it will be difficult to generate vortex waves), and make the wavelength as large as possible so that it is close to 46.4 m. At the same time, here we rotate the ship clockwise to generate a clockwise rotating vortex wave, according to theoretical calculation and laboratory results, unidirectional water surface wave propagating to the left should be generated. The field experiment results are shown in Figs. 4(a) and (b). The wave source center is set 6 m away from Luoyang Bridge, and it can be seen that the water wave on the right side of the wave source is weakened to form a unidirectional water surface wave propagating to the left.

In order to make the unidirectional water surface

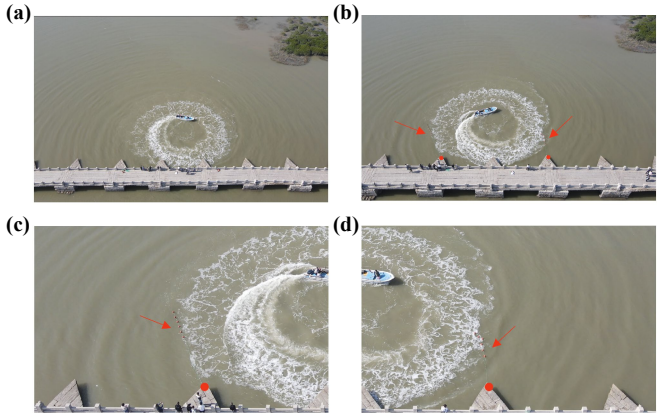

Fig. 4 Field experimental results. **(a)** Field pattern for the case when the rotating boat is close (6 m) to the real Luoyang Bridge. The boat is clockwise rotating. **(b)** Field pattern for the case when the rotating boat is close (6 m) to the real Luoyang Bridge with orange float ball. The boat is clockwise rotating. Enlarged image on the left part **(c)** and right part **(d)** of Fig. 4(b).

wave more obvious, we put two strings of orange float balls on both sides of the wave source. It can be seen that the included angle between the float ball and the vertical direction on the left side is greater than that on the right side. In order to make the deflection angle of the orange float balls look clearer, an enlarged view of the two parts of the orange float balls in Fig. 4(b) are shown in Figs. 4(c) and (d). It can be clearly seen that the left float balls have a larger included angle with the vertical direction, which proves that the strength of the water surface wave propagating to the left is greater than that propagating to the right, i.e., it forms a unidirectional water surface wave propagating to the left, which is in good agreement with our theory and laboratory results. [Figures 4(a) and (b) have corresponding videos in Section 2 of the ESM.]

4 Conclusion

We find that metagratings can also control water waves, the vortex water waves can excite unidirectional water waves near metagrating. At the same time, we calculate the equivalent anisotropic water layer model of metagrating. We verify the equivalent anisotropic water layer from analytical calculations and numerical simulations. Then we carry out experiments on a reduced metagrating and qualitatively observe the results similar to the theory. Our work provides a new method for controlling water waves, namely metagratings, which can help better understand the unidirectional propagation phenomena and physical mechanisms contained in metagratings and even in ancient building like Luoyang Bridge, it also provides a new method for bridge analysis

— using metagrating to model bridges to analyze the effect of water waves on bridges. At the same time, this discovery may contribute to ocean cargo transportation, ocean garbage cleaning, and the development and protection of ancient bridges.

Declarations The authors declare that they have no competing interests and there are no conflicts.

Electronic supplementary materials The online version contains supplementary material available at https://doi.org/10.1007/s11467-024-1411-x and https://journal.hep.com.cn/fop/EN/10.1007/s11467-024-1411-x.

Acknowledgements This work was supported by Shenzhen Science and Technology Program (Grant No. JCYJ20230807091300001), the National Natural Science Foundation of China (Grant Nos. 12374410 and 92050102), the National Key Research and Development Program of China (Grant Nos. 2023YFA1407100 and 2020YFA0710100), and the Fundamental Research Funds for the Central Universities (Grant No. 20720220033).

References and notes

1. H. Lamb, Hydrodynamics, Cambridge: Cambridge University Press, 1995
2. C. C. Mei, The Applied Dynamics of Ocean Surface Waves, Singapore: World Scientific, 1989
3. B. Wilks, F. Montiel, and S. Wakes, Rainbow reflection and broadband energy absorption of water waves by graded arrays of vertical barriers, *J. Fluid Mech.* 941, A26 (2022)
4. L. Rayleigh, On the remarkable phenomenon of crystalline reflexion described by Prof. Stokes, *Lond. Edinb. Dublin Philos. Mag. J. Sci.* 26(160), 256 (1888)
5. S. John, Strong localization of photons in certain disordered dielectric superlattices, *Phys. Rev. Lett.* 58(23), 2486 (1987)
6. E. Yablonovitch, Inhibited spontaneous emission in solid-state physics and electronics, *Phys. Rev. Lett.* 58(20), 2059 (1987)
7. J. D. Joannopoulos, P. R. Villeneuve, and S. Fan, Photonic crystals, *Solid State Commun.* 102(2–3), 165 (1997)
8. J. B. Pendry, D. Schurig, and D. R. Smith, Controlling electromagnetic fields, *Science* 312(5781), 1780 (2006)
9. U. Leonhardt, Optical conformal mapping, *Science* 312(5781), 1777 (2006)
10. H. Y. Chen, C. T. Chan, and P. Sheng, Transformation optics and metamaterials, *Nat. Mater.* 9(5), 387 (2010)
11. D. Schurig, J. J. Mock, B. J. Justice, S. A. Cummer, J. B. Pendry, A. F. Starr, and D. R. Smith, Metamaterial electromagnetic cloak at microwave frequencies, *Science* 314(5801), 977 (2006)
12. S. L. Sun, Q. He, S. Y. Xiao, Q. Xu, X. Li, and L. Zhou, Gradient-index meta-surfaces as a bridge linking propagating waves and surface waves, *Nat. Mater.* 11(5), 426 (2012)
13. N. Yu, P. Genevet, M. A. Kats, F. Aieta, J. P. Tetienne, F. Capasso, and Z. Gaburro, Light propagation with phase discontinuities: Generalized laws of reflection and refraction, *Science* 334(6054), 333 (2011)
14. M. Khorasaninejad, W. T. Chen, D. C. Devlin, J. Oh, A. Y. Zhu, and F. Capasso, Metalenses at visible wavelengths: Diffraction-limited focusing and subwavelength resolution imaging, *Science* 352(6290), 1190 (2016)
15. M. Khorasaninejad and F. Capasso, Metalenses: Versatile multifunctional photonic components, *Science* 358(6367), eaam8100 (2017)
16. G. Zheng, H. Mühlenbernd, M. Kenney, G. Li, T. Zentgraf, and S. Zhang, Metasurface holograms reaching 80% efficiency, *Nat. Nanotechnol.* 10(4), 308 (2015)
17. See the Electronic Supplemental Materials for more information.
18. X. Hu, Y. Shen, X. Liu, R. Fu, and J. Zi, Superlensing effect in liquid surface waves, *Phys. Rev. E* 69, 030201(R) (2004)
19. J. Mei, C. Qiu, J. Shi, and Z. Liu, Highly directional liquid surface wave source based on resonant cavity, *Phys. Lett. A* 373(33), 2948 (2009)
20. M. Farhat, S. Enoch, S. Guenneau, and A. B. Movchan, Broadband cylindrical acoustic cloak for linear surface waves in a fluid, *Phys. Rev. Lett.* 101(13), 134501 (2008)
21. S. Y. Zou, Y. D. Xu, R. F. Zatianina, C. Li, X. Liang, L. Zhu, Y. Zhang, G. Liu, Q. H. Liu, H. Chen, and Z. Wang, Broadband waveguide cloak for water waves, *Phys. Rev. Lett.* 123(7), 074501 (2019)
22. H. Chen, J. Yang, J. Zi, and C. T. Chan, Transformation media for linear liquid surface waves, *Europhys. Lett.* 85(2), 24004 (2009)
23. Z. Wang, P. Zhang, X. Nie, and Y. Zhang, Manipulating water wave propagation via gradient index media, *Sci. Rep.* 5(1), 16846 (2015)
24. C. Zhang, C. T. Chan, and X. Hu, Broadband focusing and collimation of water waves by zero refractive index, *Sci. Rep.* 4, 6979 (2014)
25. C. Li, L. Xu, L. Zhu, S. Zou, Q. H. Liu, Z. Wang, and H. Chen, Concentrators for water waves, *Phys. Rev. Lett.* 121(10), 104501 (2018)
26. X. Zhao, X. Hu, and J. Zi, Fast water waves in stationary surface disk arrays, *Phys. Rev. Lett.* 127(25), 254501 (2021)
27. S. Chen, Y. Zhou, Z. Wang, and H. Chen, Metagrating in ancient Luoyang Bridge, *Europhys. Lett.* 132(2), 24003 (2020)
28. Z. L. Deng, S. Zhang, and G. P. Wang, A facile grating approach towards broadband wide-angle and highefficiency holographic metasurfaces, *Nanoscale* 8(3), 1588 (2016)
29. Y. Ra'di, D. L. Sounas, and A. Alù, Metagratings beyond the limits of graded metasurfaces for wave front control, *Phys. Rev. Lett.* 119(6), 067404 (2017)
30. A. Wu, H. Li, J. Du, X. Ni, Z. Ye, Y. Wang, Z. Sheng, S. Zou, F. Gan, X. Zhang, and X. Wang, Experimental demonstration of in-plane negative-angle refraction with an array of silicon nanoposts, *Nano Lett.* 15(3), 2055 (2015)
31. R. Paniagua-Domínguez, Y. F. Yu, E. Khaidarov, S.

Choi, V. Leong, R. M. Bakker, X. Liang, Y. H. Fu, V. Valuckas, L. A. Krivitsky, and A. I. Kuznetsov, A metalens with a near-unity numerical aperture, *Nano Lett.* 18(3), 2124 (2018)
32. M. Khorasaninejad, A. Ambrosio, P. Kanhaiya, and F. Capasso, Broadband and chiral binary dielectric metaholograms, *Sci. Adv.* 2(5), e1501258 (2016)
33. P. Genevet, J. Lin, M. A. Kats, and F. Capasso, Holographic detection of the orbital angular momentum of light with plasmonic photodiodes, *Nat. Commun.* 3(1), 1278 (2012)
34. Y. Y. Cao, Y. Y. Fu, Q. J. Zhou, X. Ou, L. Gao, H. Chen, and Y. Xu, Mechanism behind angularly asymmetric diffraction in phase-gradient metasurfaces, *Phys. Rev. Appl.* 12(2), 024006 (2019)
35. N. Mohammadi Estakhri and A. Alù, Wave-front transformation with gradient metasurfaces, *Phys. Rev. X* 6(4), 041008 (2016)
36. V. S. Asadchy, M. Albooyeh, S. N. Tcvetkova, A. Díaz-Rubio, Y. Ra'di, and S. A. Tretyakov, Perfect control of reflection and refraction using spatially dispersive metasurfaces, *Phys. Rev. B* 94(7), 075142 (2016)
37. A. Epstein and G. V. Eleftheriades, Synthesis of passive lossless metasurfaces using auxiliary fields for reflectionless beam splitting and perfect reflection, *Phys. Rev. Lett.* 117(25), 256103 (2016)
38. Y. Y. Fu, C. Shen, Y. Y. Cao, L. Gao, H. Chen, C. T. Chan, S. A. Cummer, and Y. Xu, Reversal of transmission and reflection based on acoustic metagratings with integer parity design, *Nat. Commun.* 10(1), 2326 (2019)
39. Y. Ra'di, D. L. Sounas, and A. Alù, Metagratings: beyond the limits of graded. metasurfaces for wave front control, *Phys. Rev. Lett.* 119(6), 067404 (2017)
40. www.mzsluy.tw/content/2018-07/07/content_5840028.htm
41. Z. J. Dai and Q. Chen, Fujian Ancient Architecture, Beijing: People's Education Press, 2019
42. Y. Xu, Y. Fu, and H. Chen, Planar gradient metamaterials, *Nat. Rev. Mater.* 1(12), 16067 (2016)
43. L. Han, S. Chen, and H. Chen, Water wave polaritons, *Phys. Rev. Lett.* 128(20), 204501 (2022)
44. X. Hu, C. T. Chan, K. M. Ho, and J. Zi, Negative effective gravity in water waves by periodic resonator arrays, *Phys. Rev. Lett.* 106(17), 174501 (2011)
45. G. B. Airy, in: Encyclopaedia Metropolitana, edited by H. J. Rose, *et al.*, London: Taylor, 1841
46. A. D. D. Craik, The origins of water wave theory, *Annu. Rev. Fluid Mech.* 36, 1 (2004)
47. F. J. Rodríguez-Fortuño, G. Marino, P. Ginzburg, D. O'Connor, A. Martínez, G. A. Wurtz, and A. V. Zayats, Near-field interference for the unidirectional excitation of electromagnetic guided modes, *Science* 340(6130), 328 (2013)
48. F. J. Garcia-Vidal, L. Martin-Moreno, and J. B. Pendry, Surfaces with holes in them: New plasmonic metamaterials, *J. Opt. A* 7(2), S97 (2005)